Print ISSN: 0976-2876 Online ISSN: 2250-0138

Available online at: http://www.ijsr.in

INDIAN JOURNAL OF SCIENTIFIC RESEARCH

DOI:10.32606/IJSR.V16.I1.00014


Received: 12-04-2025 Accepted: 13-07-2025 Publication: 31-08-2025

Indian J.Sci.Res. 16 (1): 85-92, 2025 Original Research Article

# EVALUATING THE IMAGE QUALITY PARAMETERS OF CT-SIMULATOR USING A QUART PHANTOM

**RAHUL RAI[a1] AND KRISHNA KUMAR SINGH[b]**

[ab]Department of Physics, F.S. University, Shikohabad, Uttar Pradesh, India

## ABSTRACT

**This study aims to give medical physicists a structure and guidelines for creating a thorough Imaging Quality Assurance program for CT scanners used for CT simulation. And to ensure the safe and correct functioning of the CT-simulation process. The assessment of image quality can be carried out utilizing a phantom known as QUART phantom in order to comply with the recommendation of AAPM report Task Group No. 66. Our investigation was conducted using a Philips Incisive 128 slice CT scanner (Philips Healthcare (Suzhou) Co., Ltd., China). QUART phantom was used for image quality evaluation of CT-Simulator. The CT-Simulator's image quality control was determined by measuring and selecting the following parameters: HU accuracy, uniformity, slice thickness, LCV, noise, CNR, SNR, spatial resolution and geometric scaling. The evaluation of the QUART phantom on the CT-Simulator for the purpose of verifying image quality parameters has successfully met the standards outlined in the AAPM report from Task Group No. 66. It is strongly recommended that radiotherapy and diagnostic institutions acquire the QUART phantom to leverage its benefits in enhancing or maintaining the overall performance of their CT-Simulators or CT devices.**

**KEYWORDS:** CT-Simulator, QUART Phantom, Hounsfield Unit, Low Contrast Variability, Contrast-to-Noise Ratio, Signal-to-Noise Ratio, Spatial Resolution

Computed Tomography (CT) simulator plays a crucial to radiotherapy. Because it can generate the patients three-dimensional (3D) picture, that helps with target and organ at-risk delineation, treatment planning and dose calculation. In diagnostic CT technology, a CT simulator can have many rows of detectors. It has certain features, including a big gantry bore size, a flat tabletop, and a laser positioning system, to replicate radiation therapy equipment. CT scanners were primarily developed for diagnostic imaging, with the patient lying on a curved couch. Most CT manufacturers offer a flat top in addition to the curved couch for performing radiation applications, since radiotherapy CT simulators require a flat couch in order to mimic a treatment couch (Liu *et al.*, 2009).

In recent years, medical imaging technologies have become essential for precise diagnosis, human body visualization, and treatment planning. Existing technologies are being integrated or further enhanced, while new ones are being created. These medical imaging techniques have also contributed to the development of so-called phantoms (DeWerd and Kissick, 2014). From the ancient Greek φάντασμα (phántasma), the term "phantom" means "apparition," "ghost," or "mirage." According to the definition, a phantom in the context of medicine is a model of an organ or bodily component used for research or education. However, there is no standard definition of "phantom" in the medical literature, and this terminology is unclear (Wegner *et al.*, 2023). A phantom in medical imaging is a test specimen that, in terms of a few chosen characteristics, resembles the original clinical item. In medical imaging, a phantom is a model that replicates tissue and its characteristics. These characteristics might be qualitative, such tissue-like visual contrast, or quantitative, like X-ray attenuation coefficients. Numerous kinds of phantoms perform various functions, from teaching to quality control, or calibration. For instance, phantoms are frequently employed in radiation therapy to confirm treatment plans.

In order to ensure precise target and critical structure localization and treatment beam placement in relation to a patient's volumetric CT scans, the imaging Quality Assurance (QA) test should be performed most accurately and precisely. In CT-Simulator's Image Quality (IQ) parameters such as contrast-to-noise ratio, spatial resolution, image uniformity and noise are crucial. The American Association of Physicists in Medicine (AAPM) strongly advises that image quality be evaluated on a regular basis as per report of Task Group No. 66 (Mutic *et al.*, 2003).

This study aims to give medical physicists a structure and guidelines for creating a thorough Imaging QA program for CT scanners used for CT simulation. And to ensure the safe and correct functioning of the CT-

[1]**Corresponding author**

simulation process. The assessment of image quality can be carried out utilizing a phantom known as QUART phantom (model: QUART DVT_VN, Quality Assurance in Radiology "QUART" GmbH) (www.quart.de) in order to comply with the recommendation. The methods for measuring image quality characteristics are described in this paper.

## MATERIALS AND METHODS

Our investigation was conducted using a Philips Incisive 128 slice CT scanner (Philips Healthcare (Suzhou) Co., Ltd., China). For the purpose of CT simulation, the curved couch that comes with this CT scan is flattened using a CT overlay (Figure 1). QUART phantom was used for image quality evaluation of CT-Simulator. QUART phantom has a 160 mm diameter and is composed of Polymethyl Methacrylate (PMMA), sometimes known as acrylic. It has a lightweight and simple design. For laser alignment, the phantom is transparent and has visible white cross markings (Figure 2). For high- and low-contrast measurements with regard to PMMA, it has a centre module that is 3 cm thick and has four cylindrical holes that are 15 mm in diameter as showing in Figure 3. These holes include two air holes, one Polytetrafluoroethylene (PTFE) or Teflon hole, and one Polystyrene insert. The materials have typical Hounsfield Unit (HU) values of 120 for PMMA (body), -35 for polystyrene, 990 for Teflon and -1000 for Air cavity. The QUART phantom additionally has two 0.5 mm thick air gaps that are 30° oriented relative to the phantom axis for measuring slice thickness. Two identical, six-centimetre wide homogenous PMMA modules are installed and utilized as uniformity modules. The two six millimetres wide polycarbonate plates attached to both cylindrical faces to provide solid installation on the couch's surface. This phantom can directly test HU accuracy, slice thickness, Contrast-to-Noise Ratio (CNR) and Low Contrast Variability (LCV) using materials inserted. For image uniformity, Signal-to-Noise Ratio (SNR), Noise, spatial resolution and geometrical scaling measurement with homogenous modules.

A QUART phantom was put over the CT flat couch between H2 and H3 indexing to perform IQ) assurance test measurements, as seen in Figure 4. The goal was to verify the CT laser's positioning accuracy. QUART phantom has a groove on its body with a visible white cross marking to aid with alignment. If the locations of any of the lasers on either side changes, this phantom can detect it in extremely simple way. Thereafter, a CT scan is taken of 3mm slice thickness using 120 kV of applied potential. The CT-Simulator's image quality control was determined by measuring and selecting the following parameters: HU accuracy, uniformity, slice thickness, LCV, Noise, CNR, SNR, spatial resolution and geometric scaling.

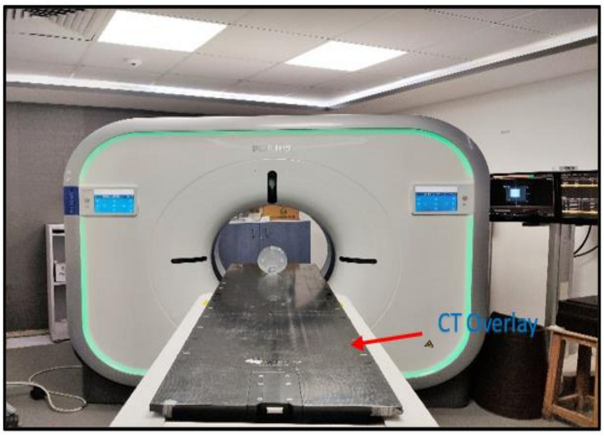


**Figure 1: Showing the picture of CT-Simulator with CT Overlay**

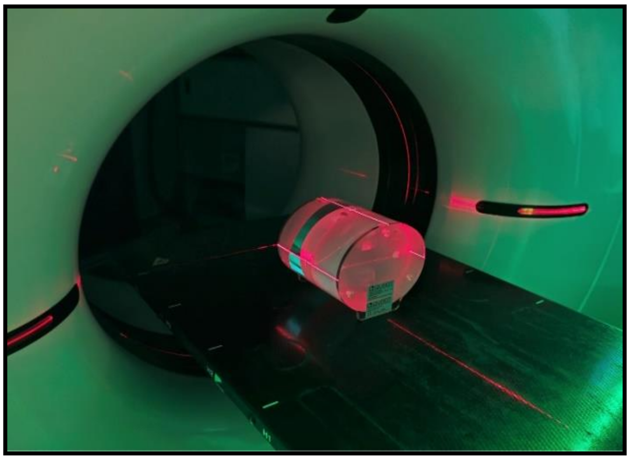

**Figure 2: Showing QUART phantom align with the CT lasers**

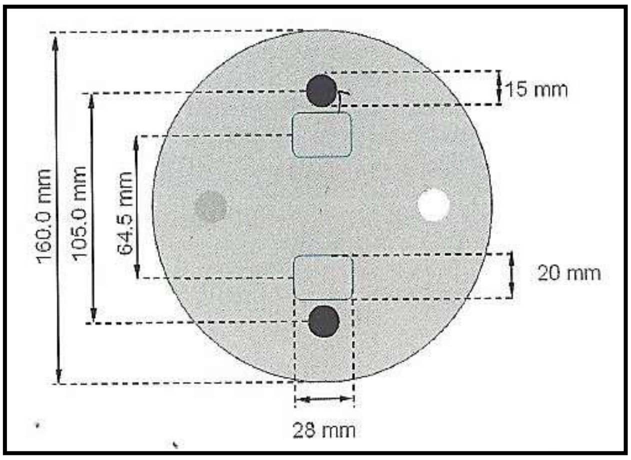


**Figure 3: A schematic drawing of the central module of the QUART phantom**

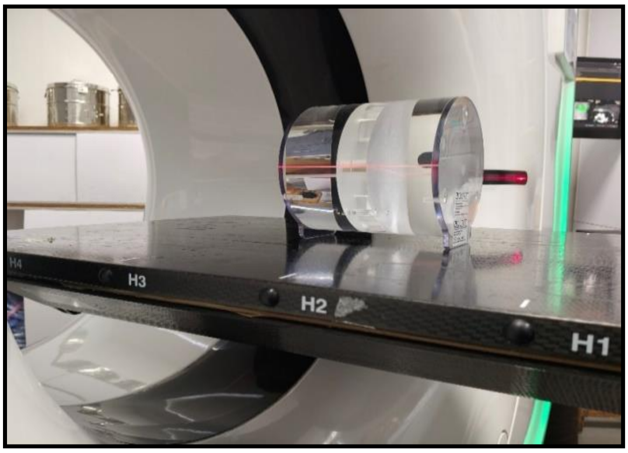


**Figure 4: Showing QUART Phantom placed between H2 and H3 Indexing**

### HU Accuracy Measurement

By evaluating the mean HU values of the QUART phantom in distinct Regions of interest (ROIs) with different materials, such as body (Acrylic), Teflon, Polystyrene, and the two air holes we can assess the HU accuracy of a reconstructed CT scans (Figure 5). A slice that was well-centered had been chosen for this test. The Eclipse Treatment Planning System TPS V.15.06, which enables the measurement of the average HU value in the chosen ROIs, had been used to manage the chosen slice. For the measurement, three distinct materials have been used: Teflon, Polystyrene, and Acrylic. By using the Eclipse Histogram tab, a ROI of 7x7 mm was drawn in each selected material as shown in Figure 6. A comparison has been made between the theoretically expected values stated by manufacturers as shown in Table 1 and the measured mean values that the Eclipse yields. HU accuracy is defined as the discrepancies between the observed average and the stated values with a tolerance of ±50HU.

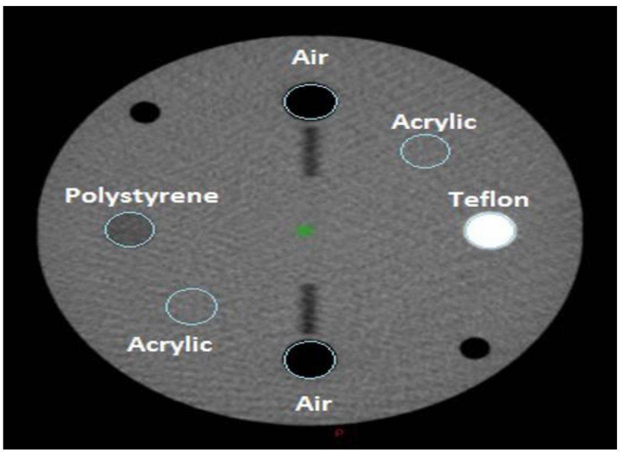


**Figure 5: Location of QUART phantom Inserts**

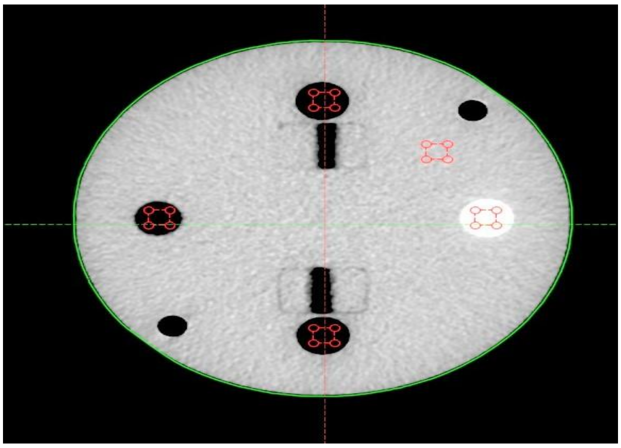

**Figure 6: Showing ROI of 7x7 mm was drawn in each selected material**

### Image Uniformity Measurement

Through this process, the reconstructed volume's image uniformity (maximum deviation between center and boundary ± 50 HU) was confirmed. It may be measured in one of the two homogeneous modules, each 6 cm thick, that surround the QUART phantom's core module. For this measurement an image slice of homogeneous area of a QUART phantom, approximately 4cm away from the central slice containing the HU inserts. Using Histogram tool, a ROI of 20x20 mm size is created and placed at different places to measure the mean HUs, one at the center and four peripheral regions of the phantom as shown in Figure 7.

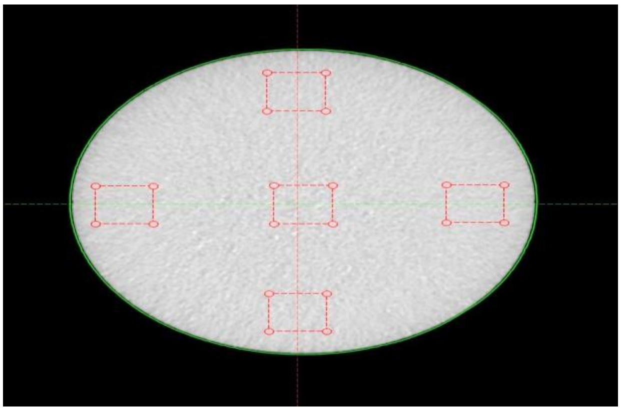

**Figure 7: Showing homogeneous slice ROI of 20x20 mm one at the centre and four at peripheries**

### Noise, Signal-to-Noise Ratio (SNR) and Contrast-to-Noise Ratio (CNR)

Noise represents the local statistical fluctuation (standard deviation) of CT or HU numbers of a homogeneous ROI. This measurement was done in the homogeneous region at 4 cm from the central slice by creating a ROI of 20x20mm size at its center as shown in Figure 8 with a tolerance of ±15%.

The signal-to-noise ratio (SNR), plays a key concept in radiological physics which compares the intended signal level to the background noise level to determine the quality level of an image. SNR was measured in the homogeneous region of QUART phantom same as the Noise as shown in Figure 8. In terms of mathematics, SNR is the ratio of the average signal strength (HU value) to the standard deviation ($\sigma$) of noise:

SNR= Mean Signal (HU Value)/ standard deviation ($\sigma$)

The difference in HU values between an insert and the surrounding material, divided by the noise, yields the CNR value, which indicates the overall quality of an image.

$$\mathrm{CNR} = \frac{[\mathrm{abs}\ (\mathrm{HU\ insert} - \mathrm{HU\ background})]}{(\sigma 2\ \mathrm{insert} + \sigma 2\ \mathrm{background})^{1/2}}$$

This measurement was taken at the central slice by creating a ROI of 7x7 mm size at the Acrylic (background) and Polystyrene(insert) materials and measuring their mean HUs and standard deviations ($\sigma$) as shown in Figure 9.

**Low Contrast Variability (LCV) Measurement**

To measure the image quality LCV was measured by using following equation proposed by Elstrøm *et al.* ( 2011), in his study two inserts with very small difference in mass density and HU values were placed in the phantom. Where the HU values were (1.05 g/cm3 and 0.92 g/cm3) respectively and mass density of low-density polyethylene and polystyrene were (-100 HU and -35 HU) respectively.

$$\mathrm{LCV} = \frac{2.75\ (\sigma 2\ + \sigma 2)}{\mathrm{P1} - \mathrm{P2}}$$

Where P1 and σ1are the mean pixel (HU) and standard deviation value of a region of interest inside the polystyrene insert and P2 and σ2 are the mean pixel (HU) and SD value of a region of interest inside the polyethylene insert. This measurement was taken at the central slice by creating a ROI of 7x7 mm size at the Acrylic (PMMA) and Polystyrene materials and measuring their mean HUs and standard deviations ($\sigma$) as shown in Figure 9.

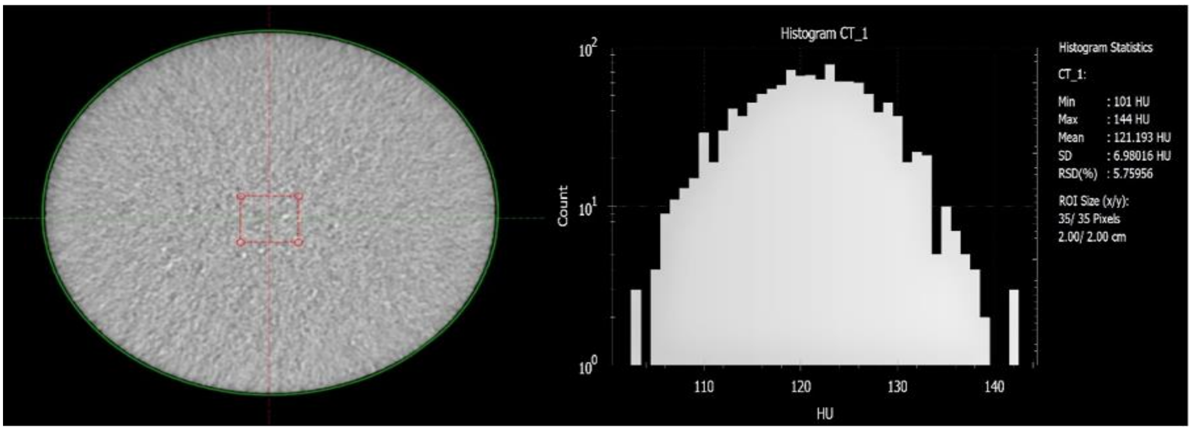


**Figure 8: Showing a ROI of 20x20 mm at the center of homogeneous slice and Histogram chart for measurement of Noise and SNR**

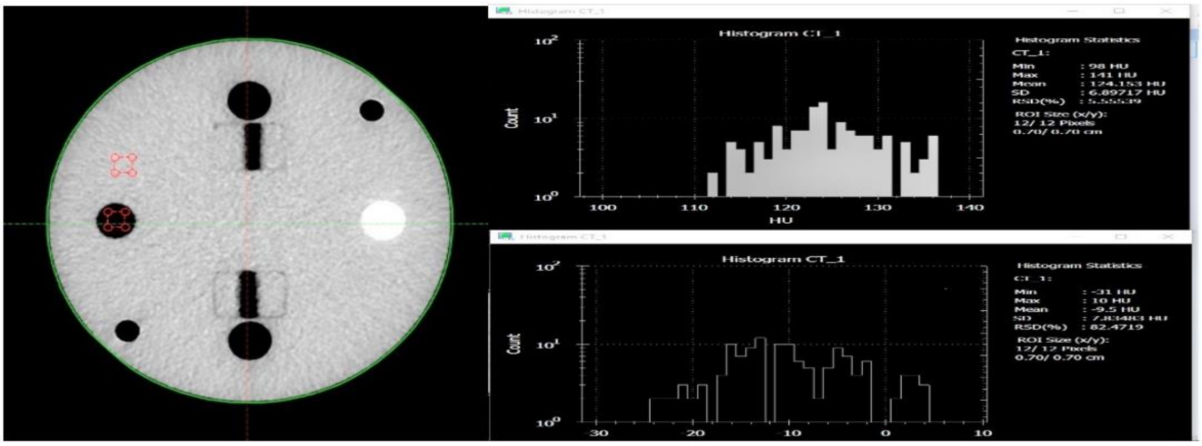


**Figure 9: ROI of 7x7 mm size at the Acrylic (background) and Polystyrene (insert) materials and measuring their mean HUs and standard deviations for CNR and LCV**

### Slice Thickness Measurement

Assessing the geometry of a slanted structure in a single created slice serves as the basis for measuring slice thickness. By measuring the Full Width of Half Maximum (FWHM) of a profile, one may ascertain the slice thickness.

Slice Thickness (S) = tan(α) * FWHM

An angled air gap is used to measure the slice thickness in QUART phantom. There is a 0.5 mm wide air gap in the QUART phantom. Since there is a 30° inclination angle, the slice width may be determined by:

Slice Thickness (S) = 0.577 * FWHM

An air gap and a well-centered slice have been chosen for this test. The area profile was of 20 mm high and 28 mm width was taken to find out the FWHM as shown in the Figure 10 with a tolerance of ±1mm.

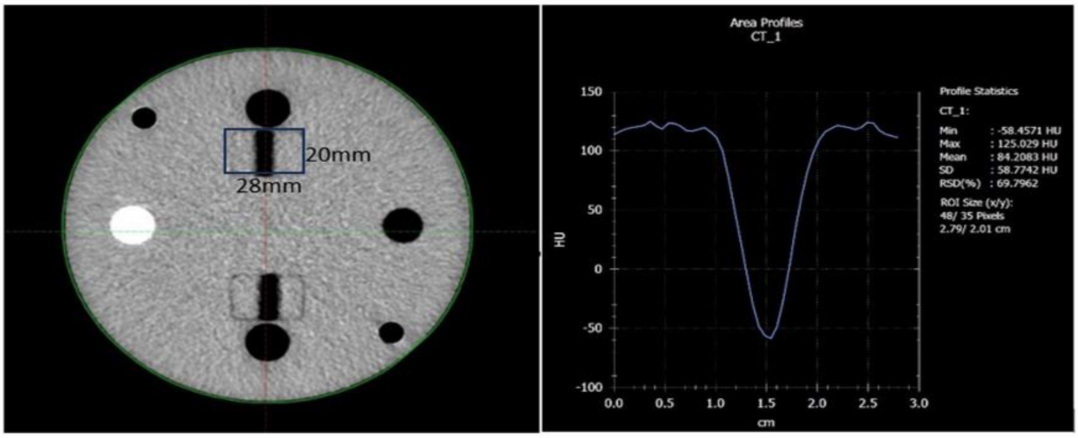


**Figure 10: Showing the area profile of 20 mm high and 28 mm width was drawn to find out the FWHM using a curve**

### Geometric Scaling Measurement

The QUART phantom measures 160 mm in diameter. By measuring the diameter in both horizontal and vertical directions by setting the window level to within value of "-1000 to +200" HU in order to display mid-grey roughly as the average between air and the phantom body, the geometric scaling may be confirmed with a tolerance of ±1mm as shown in Figure 11.

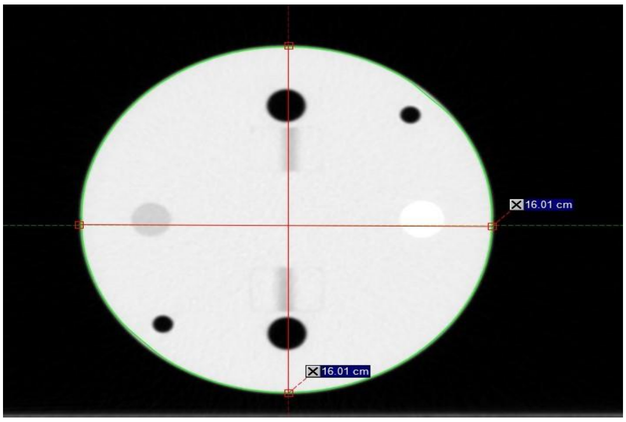


**Figure 11: Showing Vertical and Horizontal diameter measurements**

### Spatial Resolution Measurement

The HU profiles that are perpendicular to the QUART phantom boundary are used to assess the spatial resolution directions by setting the window level to within value of "-1000 to +200" HU. The test's spatial resolution is determined by the phantom edge's width, which cannot be greater than 1.7 mm. By measuring the width of the penumbra of the edge profile, one may find the resolution of the phantom. A profile is produced using a rectangular ROI at the phantom's right edge, measuring and reporting the distance between the profile points at -700 and -200 HU. The ROI is 1 cm high and 0.5 cm wide. The identical procedures are followed for the vertical direction with the ROI being the phantom's upper edge as shown in the Figure 12.

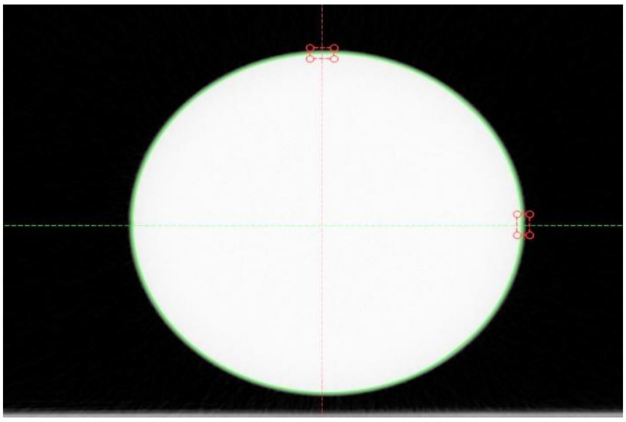

**Figure 12: Showing spatial resolution measurement using ROI of 1 cm and 0.5 cm horizontally and vertically**

## RESULTS AND DISCUSSIONS

Imaging quality tests should be performed routinely for a CT-Simulator based on regular measurements and evaluation of the constancy of these quality parameters of the image a baseline can be established in any radiotherapy or diagnostic centre. According to some authors, tolerances should be set at the baseline value at acceptance plus or minus three times the standard deviation(Chan *et al.*, 2011; Stock *et al.*, 2009).This study recommends that several scans under the same conditions should yield baseline values for the various image quality characteristics as an average over different slices.

### HU Accuracy Measurement

The theoretically predicted values of the materials in the identical ROIs, as indicated in Table 1, have been compared with all measured values. The results demonstrate that empirically measured HU levels correlate to established theoretical values.

**Table 1: Showing theoretically values stated by manufacturers and the measured mean HU values**

| Materials | Theoretical HU Values | Measured HU Values |
|---|---|---|
| Polystyrene | -35 | -9.50 |
| Teflon | 990 | 943.00 |
| Acrylic | 120 | 123.85 |
| Air | -1000 | -987.69 |

### Image Uniformity Measurement

Table 2 shows the results according to the homogeneity. These findings demonstrate the HU values recorded in the ROIs of the four peripheries and the center of a homogeneous slice. An indicator of image uniformity is the consistency of HU values from the ROI center to the ROI boundaries of the image slice of a uniform density material. According to a study done by M.Maqbool the difference in the mean HU between a peripheral and a central region of a homogeneous slice with < 8HU is in good agreement (Maqbool, 2017). Our study showed that the difference between the HU values at the center and peripheries are within ±4HUs.

### Noise, Signal-to-Noise Ratio (SNR) and Contrast-to-Noise Ratio (CNR)

The distribution of HU values (minimum to maximum) for the ROI of the homogenous slice is shown in Figure 8. The Image noise is given by the standard deviation of the HU values which was found to be 5.76%. Higher the percentage of noise in the image, poorer will its quality. Many studies showed that the denoising methods should be performed to improve the image quality for more accurate diagnosis (Diwakar & Kumar, 2018).

For SNR the value was measured to be 17.36 from Figure 8. SNR is essential in medical imaging since it directly impacts how visible diagnostic data is. A lower SNR produces a grainy or distorted image that may hide most critical details from an image, a higher SNR shows a sharper image with more detailed information which is a need for any CT-Scanner or CT-Simulator (Mahesh, 2013).

Table 3 shows the analysis of CNR of the selected slices where values was found to be 12.80. In general, the larger the CNR value, lesser noise will be observed in an image and the quality will be improved. On other hand, the lowest CNR value, greater will be the noise in the images and image quality will be degraded.

### Low Contrast Variability (LCV) Measurement

Table 4 shows the calculated values of low contrast variability which was found to be 0.35%. The image noise has a direct correlation with the low contrast visibility. An image with a lower LCV value shows greater soft tissue imaging, reduced noise, and superior distinction between areas with slight density variations. A study by Stock *et al.* demonstrated that the factors in the imaging protocols affected the fluctuation of LCV values. Specifically, lowering the mA or kV settings resulted in both an increase in LCV and a decrease in uniformity index (Stock *et al.*, 2009).

### Slice Thickness Measurement

An area profile has been shown in Figure 10. In our study, the FWHM was 5.0 mm and the incline angle is 30° as described before. Therefore, the slice thickness was calculated as 2.9 mm (vs 3.0 mm as expected). The baseline value was close to the nominal value of 120 HU for PMMA material, with a minimum at -58.45 HU.

### Geometric Scaling Measurement

The geometric scaling has been verified by measuring the diameter both in horizontal and vertical direction as shown in Figure 11. The diameter of the phantom was 160.1mm and 160.1mm vertically and horizontally respectively. The accuracy of scaling measurement within ±1mm the accuracy of measurement is in agreement with the value that was recommended by the manufacturer.

### Spatial Resolution Measurement

From the Figure 13 we have obtained the spatial resolutions for horizontal and vertical edges of QUART phantom which were 1.05 mm and 0.95 mm. The accuracy of spatial resolution was ≤ 1.7 mm as specified by the manufacture.

**Table 2: HU uniformity values of different ROIs**

| HU uniformity | HU Values (A) | HU Value At Center (B) | HU Difference (A-B) |
|---|---|---|---|
| ROI Left | 123.00 | 122.37 | 0.63 |
| ROI Top | 122.50 | | 0.13 |
| ROI Right | 123.25 | | 0.88 |
| ROI Bottom | 122.40 | | 0.03 |

**Table 3: Shows the analysis of the Contrast-to-Noise Ratio (CNR)**

| Materials | HU Values | Standard Deviation (SD) | CNR |
|---|---|---|---|
| Polystyrene | -9.5 | 7.83 | 12.80 |
| Acrylic | 124.15 | 6.89 | |

**Table 4: Shows the analysis of the Low contrast variability (LCV)**

| Materials | HU Values | Standard Deviation (SD) | LCV % |
|---|---|---|---|
| Polystyrene | -9.5 | 7.83 | 0.35% |
| Acrylic | 124.15 | 6.89 | |

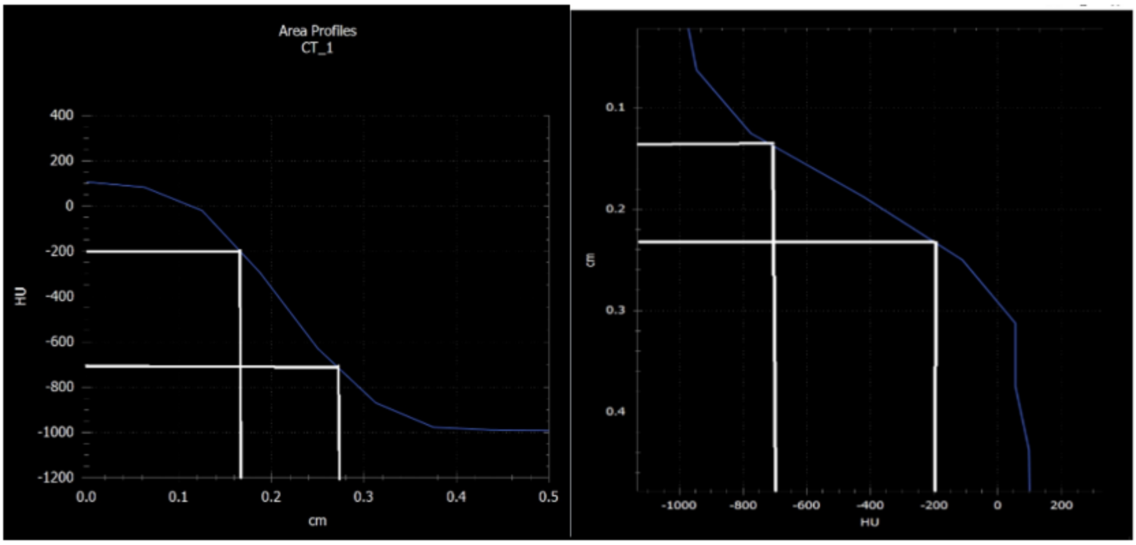


**Figure 13: Showing Horizontal and Vertical profiles**

## CONCLUSION

The evaluation of the QUART phantom on the CT-Simulator for the purpose of verifying image quality parameters has successfully met the standards outlined in the AAPM report from Task Group No. 66. This study clearly demonstrates that the QUART phantom performs comparably to other phantoms available in the market for the purpose of image quality validation.

The QUART phantom is designed to be lightweight, facilitating ease of transport, enabling rapid measurements, and providing a reliable tool for deriving imaging parameters of a CT-Simulator. It is strongly recommended that radiotherapy and diagnostic institutions acquire the QUART phantom to leverage its benefits in enhancing or maintaining the overall performance of their CT-Simulators or CT devices. Consequently, we advocate that institutions incorporate the QUART phantom into their routine quality assurance protocols to achieve greater accuracy and precision in testing.

## ACKNOWLEDGEMENT

Authors are thankful to Raj Scanning Ltd. (Lucknow Cancer Institute), Lucknow, Uttar Pradesh, India for providing necessary facilities and cooperation.

## REFERENCES

Chan M., Yang J., Song Y., Burman C., Chan P. and Li S., 2011. Evaluation of imaging performance of major image guidance systems. Biomedical Imaging and Intervention Journal, **7**(2): e11. https://doi.org/10.2349/biij.7.2.e11

DeWerd L.A. and Kissick M., 2014. The Phantoms of Medical and Health Physics. Springer New York. https://doi.org/10.1007/978-1-4614-8304-5

Diwakar M. and Kumar M., 2018. A review on CT image noise and its denoising. Biomedical Signal Processing and Control, **42**: 73–88. https://doi.org/10.1016/j.bspc.2018.01.010

Elstrøm U.V., Muren L.P., Petersen J.B.B. and Grau C., 2011. Evaluation of image quality for different kV cone-beam CT acquisition and reconstruction methods in the head and neck region. Acta Oncologica, **50**(6): 908–917. https://doi.org/10.3109/0284186X.2011.590525

Liu R.R., Prado K. and Gillin M., 2009. Simplified "on-couch" daily quality assurance procedure for CT simulators. Journal of Applied Clinical Medical Physics, **10**(3): 49–55. https://doi.org/10.1120/jacmp.v10i3.2844

Mahesh M., 2013. The Essential Physics of Medical Imaging, Third Edition. Medical Physics, **40**(7). https://doi.org/10.1118/1.4811156

Maqbool M., 2017. An Introduction to Medical Physics. Springer International Publishing. https://doi.org/10.1007/978-3-319-61540-0

Mutic S., Palta J.R., Butker E.K., Das I.J., Huq M.S., Loo L.-N.D., Salter B.J., McCollough C.H. and Van Dyk J., 2003. Quality assurance for computed-tomography simulators and the computed-tomography-simulation process: Report of the AAPM Radiation Therapy Committee Task Group No. 66. Medical Physics, **30**(10): 2762–2792. https://doi.org/10.1118/1.1609271

Stock M., Pasler M., Birkfellner W., Homolka P., Poetter R. and Georg D., 2009. Image quality and stability of image-guided radiotherapy (IGRT) devices: A comparative study. Radiotherapy and Oncology : Journal of the European Society for Therapeutic Radiology and Oncology, **93**(1): 1–7. https://doi.org/10.1016/j.radonc.2009.07.012

Wegner M., Gargioni E. and Krause D., 2023. Classification of phantoms for medical imaging. Procedia CIRP, **119**: 1140–1145. https://doi.org/10.1016/j.procir.2023.03.154

www.quart.de. (n.d.).